

# Multi-ion emission from large and massive keV cluster impacts

R.D. Rickman, S.V. Verkhoturov\*, G.J. Hager, E.A. Schweikert\*\*

*Department of Chemistry, Center of Chemical Characterization and Analysis, Texas A&M University, College Station, TX 77843-3144, USA*

Received 13 May 2005; received in revised form 22 June 2005; accepted 22 June 2005

Available online 2 August 2005

## Abstract

We report the first measurements of the distributions of the number of molecular ions emitted per gold cluster impact. Experiments were performed in the event-by-event bombardment/emission mode. Targets of phenylalanine were bombarded with 28.6 keV  $\text{Au}_9^+$  and 134.6 keV  $\text{Au}_{400}^{4+}$  projectiles. The secondary ions were identified with a linear time-of-flight mass spectrometer equipped with an 8-anode detector, thus allowing to record the co-emission of up to 8 phenylalanine ions. We describe how the experimentally measured molecular ion distribution is related to the initial distributions of ionized and neutral molecules.

© 2005 Elsevier B.V. All rights reserved.

**Keywords:** Gold clusters; Secondary ion mass spectrometry; Intact molecules; Multi-ion emission

## 1. Introduction

The occurrence of ion “multiplicity”, i.e., the emission of multiple ions from the impact of a keV projectile on a surface, is a well-documented observation, e.g., [1–3]. In particular, bombardment with keV polyatomic projectiles can result in a notable subset of collision cascades where multiple ions are co-emitted [4]. It has been noted that co-emission from a single projectile impact represents the ultimate spatial limit for particle-based surface analysis [5]. We lack, however, insight into these information-rich emission events. Fundamental questions remain to be addressed. Are there “exit” conditions that affect the probability of co-emission of multiple ions? What does the co-emission of multiple molecular ions reveal about the distribution of the corresponding neutral molecules? Are individual emission events, under replicate impact and target conditions, distinctly unique or, on average, equivalent events?

## 2. Experimental

In the present study we report on experiments with large and massive gold clusters, i.e., conditions with notable co-emission of multiple ions. The observations were made in the event-by-event bombardment-detection mode at the *limit of single projectile impacts*. With this approach we can unfold the co-emission of multiple ions and extract data pertinent to the questions raised above. The experiments were carried out in two different bombardment regimes involving distinct momentum effects and energy densities. Targets of deuterated phenylalanine (Aldrich 49, 014-8,  $M_w = 173.26$ ) were bombarded with large and massive gold clusters,  $\text{Au}_9^+$  of 28.6 keV and “ $\text{Au}_{400}^{4+}$ ” of 134.6 keV, respectively. “ $\text{Au}_{400}^{4+}$ ” refers to an average of projectiles with mass-to-charge ratios,  $m/q$  of  $\sim 20,000$  and an overall net charge,  $q$ , of +4 [6].

The experiments were run on a setup comprising a liquid metal ion source, a Wien filter for primary ion mass selection, a beam pulser for single projectile bombardment and a linear time-of-flight mass spectrometer [4,6,7]. The liquid metal ion source (LMIS), procured from the Institute of Nuclear Physics Orsay (France) produces gold clusters in wide range of masses [6]. The reference just cited gives details on the production and identification of heavy gold clusters. The LMIS used in this study is a duplicate of the one described in [6],

\* Corresponding author. Tel.: +1 979 845 2344; fax: +1 979 845 1655.

\*\* Corresponding author.

E-mail addresses: [verkhoturov@mail.chem.tamu.edu](mailto:verkhoturov@mail.chem.tamu.edu) (S.V. Verkhoturov), [schweikert@mail.chem.tamu.edu](mailto:schweikert@mail.chem.tamu.edu) (E.A. Schweikert).

regarding the ion source (tungsten needle and metal containing reservoir), extraction electrode and two focusing lenses. The protocol followed for producing the large cluster ions was the same as described in [6]. Generally, the emission of larger cluster ions requires a higher emission current (higher potential applied to extraction electrode) and, consequently, optimization of the values of voltages applied on the two focusing lenses.

For the mass selection of the primary cluster ions we used a Wien filter, or a combination of the Wien filter with subsequent further selection by time-of-flight. The output from the Wien filter scanned across a 0.2 mm collimator allowed to separate Au clusters up to  $\sim 1800$  amu (corresponding to  $\text{Au}_9^+$ ). Beyond  $\text{Au}_9^+$ , the output from the Wien filter appeared as a continuum of unresolved masses with a maximum of intensity at the mass  $\sim 20,000$  amu (corresponding to “ $\text{Au}_{400}^{4+}$ ”). It may be recalled that the performance of the Wien filter depends on its combined ability as a mass dispersion device and a velocity analyzer. The mass scan mentioned above is a sum of convolution integrals for different masses. Each integral is a convolution of a kinetic energy distribution of the emitted ion and a kinetic energy resolution function of the spectrometer. The resolution function depends on the size of the emission area of secondary ions, diameter of the collimator placed in front of target, and optical aberrations [8]. Although the mass separation of the primary cluster ions achieved by Wien filter is modest, it was adequate when followed by a selection based on time-of flight. The time-of flight selection of the primary cluster ions was performed with two pulse generators, specifically, a high voltage pulser and a gate generator. The high voltage generator was used to operate in the regime of single projectile bombardment. [7]. The gate generator set a time window to edge the continuum of masses around mass  $\sim 20,000$  amu. In practice, we set the Wien filter at mass 20,000 amu, and monitored the arrival of projectiles on target by the detection of secondary electrons emitted from target [7]. In a second step, the pulser (repetition rate  $\sim 1000$  pulse/s) was activated with the pulses serving as start signals for the additional time-of-flight mass selection. Under these conditions the time-of-flight spectrum of the projectiles is a single peak (Wien filter selection) with a maximum on the mass 20,000 amu, and with the corresponding flight time. To still impress the mass resolution, a gate generator was used. The latter allows to detect only projectiles which strike target at time corresponding to the mass 20,000 amu within an experimentally defined narrow time window.

The ions were detected with a dual micro-channel plate, MCP, assembly with 8-anodes provides the capability of recording, simultaneously, up to eight ions of the same  $m/q$ , provided they strike separate anodes. Cross-talk among anodes was determined to be  $<0.1\%$  [7]. All events are collected and stored as a “total matrix of events” (TME), described elsewhere [5,7]. The TME acquisition method enables one to select events by the number of ions,  $n^-$ , detected per event and extract mass spectra, which are cor-

responding to different values of  $n^-$ . For instance, when selecting  $n^- = 1$ , one obtains a mass spectrum of single ion emission events.

### 3. Results and discussion

The total spectra of the secondary ions detected from phenylalanine bombarded by 28.6 keV  $\text{Au}_9^+$  and 134.6 keV  $\text{Au}_{400}^{4+}$  ions are presented in Fig. 1a and b. These spectra are the sum of the spectra corresponding to different  $n^-$  ions selected per event, i.e., they are equivalent to spectra, which are obtained using conventional mass spectrometry. The only difference is that the eight-anode detector allows for the recording of up to eight ions with the same  $m/q$  arriving simultaneously. The yield, i.e., intensity/projectile, measured for the phenylalanine molecular ion  $\text{Ph}^-$   $[\text{M-H}]^-$  ( $m/e = 172$ ) is high and equal to  $\sim 0.93$  for the case of 134.6 keV  $\text{Au}_{400}^{4+}$  bombardment.

The co-emission of multiple ions can be described with a “multiplicity report”, i.e., the distribution of the number of

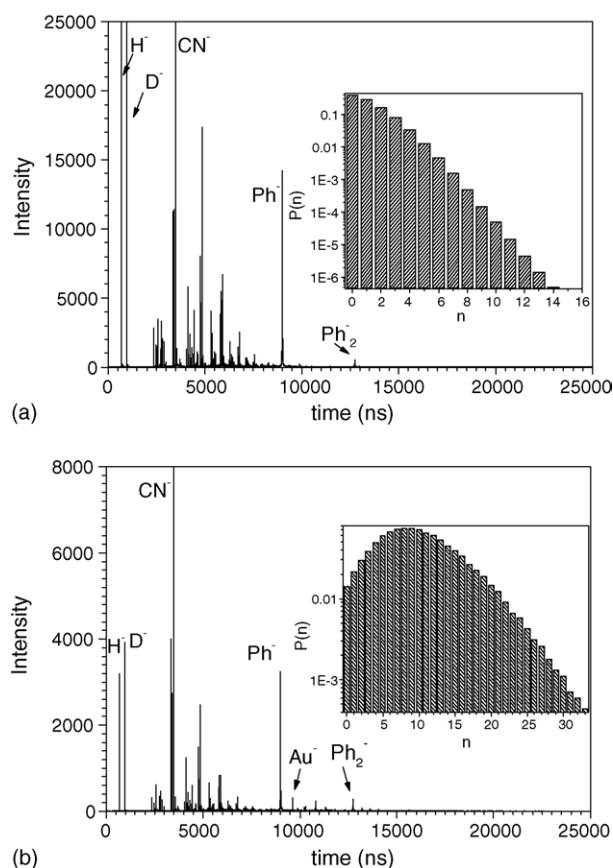


Fig. 1. Negative ion ToF mass spectra of deuterated phenylalanine from: 28.6 keV  $\text{Au}_9^+$  (a) and 134.6 keV  $\text{Au}_{400}^{4+}$  (b) bombardment. The dose of bombardment was  $\sim 10^5$  projectiles/ $\text{mm}^2$  for  $\text{Au}_{400}^{4+}$  and  $\sim 5 \times 10^6$  projectiles/ $\text{mm}^2$  for  $\text{Au}_9^+$ . The insets show the “multiplicity reports” i.e., number of ions detected per projectile impact, for  $\text{Au}_9^+$  (a) and  $\text{Au}_{400}^{4+}$  (b).

ions detected per event,  $P(n^-)$ . The insets in Figs. 1a and b show these distributions. They include all ions generated from bombardment with  $\text{Au}_9^+$  or  $\text{Au}_{400}^{4+}$  respectively. The latter induces abundant multi-ion emission; the average number of detected ions (atomic, fragment, molecular and cluster ions) per event is 10. In case of the  $\text{Au}_9^+$ , one ion is detected on average per projectile impact.

Another aspect of multi-ion emission concerns the exit conditions. Are the ions affected by Coulomb repulsion/explosion? This phenomenon is well documented for highly charged molecules or in molecular size surface areas carrying multiple charges [9–11]. The intensity of repulsion can be determined by comparing the shapes of the  $\text{Ph}^-$  peaks of mass spectra corresponding to successive values of  $n^-$ . A simple calculation of the ion time shift via repulsion within the ToF space indicates that the effect of the repulsion will be detectable when the relative potential energy of the ions at the surface emission area exceeds 1 eV. In this case, a  $\text{Ph}^-$  peak from large  $n^-$  events would be broader than a peak from events where  $n^-$  is small. The relevant peak shapes are presented in Fig. 2a and b. The superimposed  $\text{Ph}^-$  peaks correspond to the spectra where  $n^- = 1$  and 5, for the case of

the  $\text{Au}_9^+$  projectile, and  $n^- = 5, 11, 15$  and 20 for  $\text{Au}_{400}^{4+}$ . It should be noted that the spectrum with 20 ions per event includes any combination of ions with at least one  $\text{Ph}^-$ . The similarity of the peak shapes suggests that the Coulomb repulsion is minimal for the cases of the multi-ion emission considered here. This is due to the random spatial distribution of the different negative ions at the emission surface area, which possibly exceeds 10 nm [12].

A further topic of interest concerns the characteristics of co-emitted ions of the same type. We consider here the simultaneous emission of  $\text{Ph}^-$  ions, where  $k_{\text{exp}}^-$  represents the number of simultaneously detected  $\text{Ph}^-$  ions. Fig. 3a and b shows the mass spectra of the  $\text{Ph}^-$  ions ( $k_{\text{exp}}^- = 1, 2$  or 3). There is a clear correlation between the number of  $\text{Ph}^-$  ions per event  $k_{\text{exp}}^-$  and the position of the peak on the time scale. The time shift  $\Delta t$  towards shorter flight times indicates that ions with large  $k_{\text{exp}}^-$  have relatively large translational velocities. The typical experimental  $\Delta t$  is  $\sim 1$  ns. The relative kinetic energy shift  $\Delta E/E$  corresponding to successive  $\Delta t$ , is  $\sim 0.25$ . This observation may be explained with a dependence of the ionization probability  $\alpha(E)$  on the kinetic energy of the emitted particles  $E$ . An exponential or power law dependence of

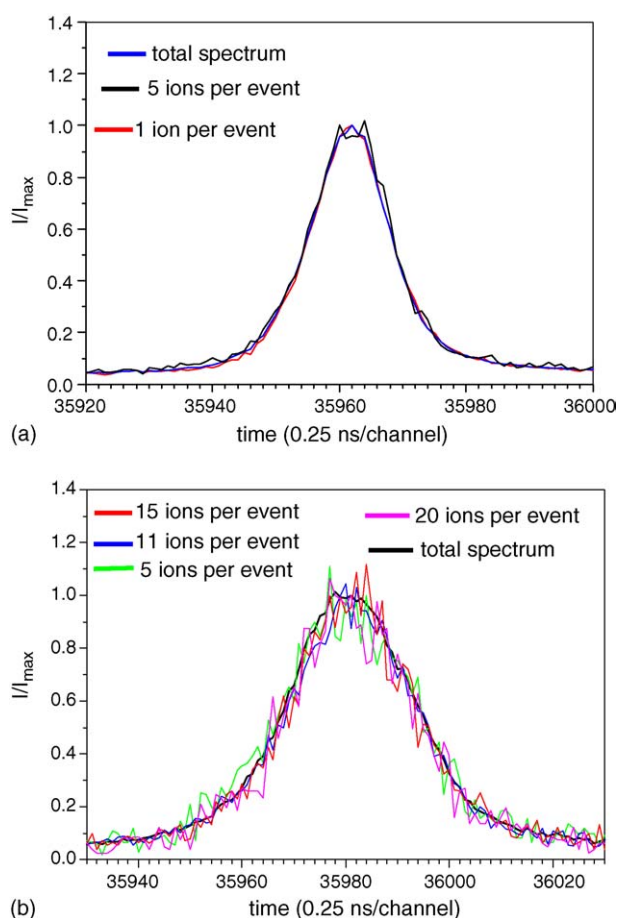


Fig. 2. Superimposed  $\text{Ph}^-$  peaks selected from the spectra with:  $n^- = 1$ , and 5 for the case of the  $\text{Au}_9^+$  projectile (a) and  $n^- = 5, 11, 15$  and 20 for the  $\text{Au}_{400}^{4+}$  (b).

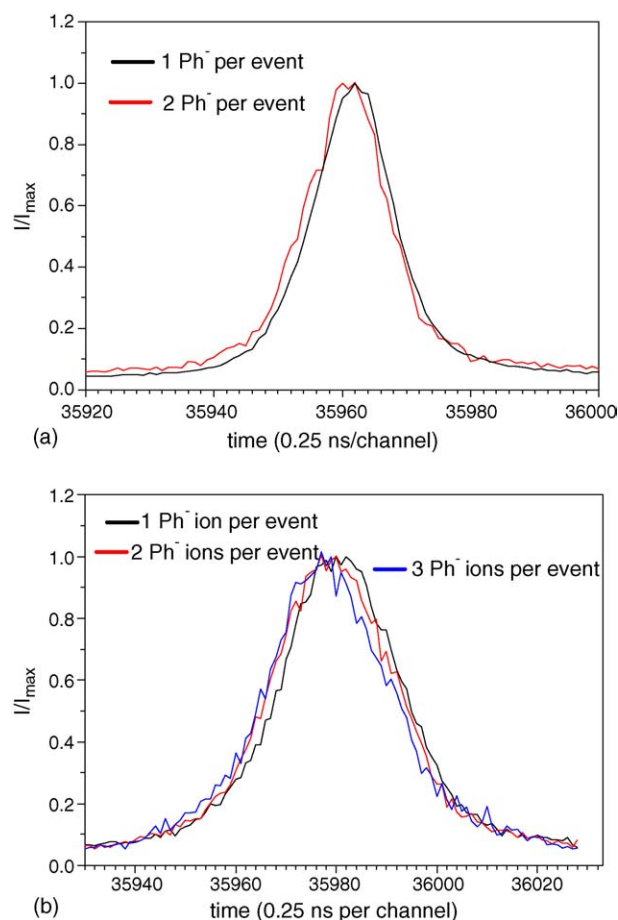


Fig. 3. Superimposed  $\text{Ph}^-$  peaks are selected from the spectra with:  $k_{\text{exp}}^- = 1$ , and 2 for the case of 28.6 keV  $\text{Au}_9^+$  (a) and  $k_{\text{exp}}^- = 1, 2$  and 3 for 134.6 keV  $\text{Au}_{400}^{4+}$  (b).

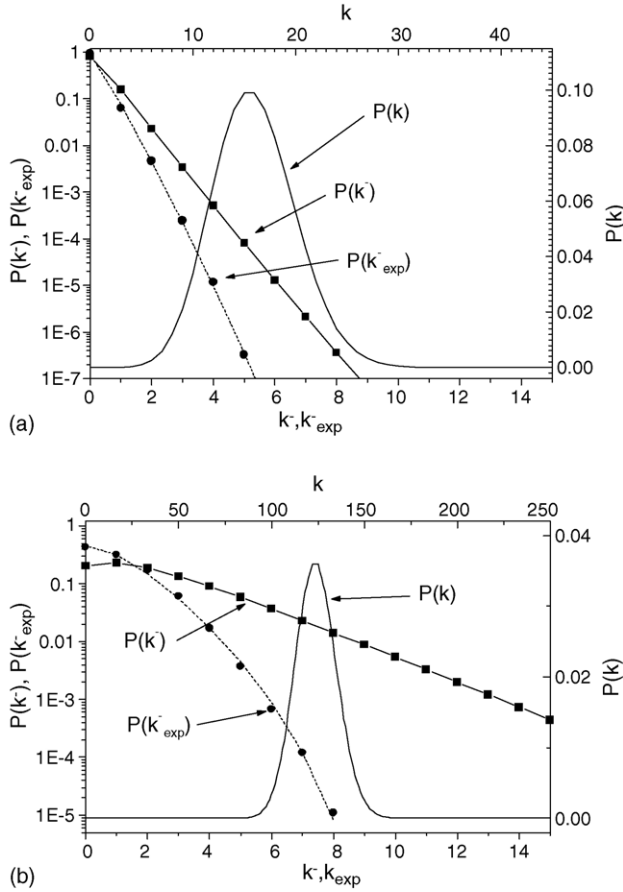


Fig. 4. The experimental distribution  $P(k_{\text{exp}}^-)$ , and distributions,  $P(k^-)$ , and  $P(k)$  calculated setting:  $Y\alpha_1 = 0.16$  for 28.6 keV  $\text{Au}_9^+$  (a) and  $Y\alpha_1 = 1.24$  for 134.6 keV  $\text{Au}_{400}^{4+}$  (b). For data from of  $\text{Au}_9^+$ , the margins of error in the values of  $P_{\text{exp}}(k_{\text{exp}}^-)$  are  $\pm 5\%$  for  $k_{\text{exp}}^- \leq 4$ , and  $\pm 15\%$  for  $k_{\text{exp}}^- = 5$  (a). For data from  $\text{Au}_{400}^{4+}$ , the margins of error in the values of  $P(k_{\text{exp}}^-)$  are  $\pm 2.5\%$  for  $k_{\text{exp}}^- \leq 5$ , and  $\pm 10\%$  for  $6 \leq k_{\text{exp}}^- \leq 8$  (b). The dashed line on the experimental  $P(k_{\text{exp}}^-)$  is a least-square fit with the model explained in the text. The ionization probability was set arbitrarily at  $\alpha_1 = 0.01$ .

$\alpha(E)$  on the emission velocity is predicted by different models and was observed experimentally [13–15]. It is not clear which mechanism of ionization is relevant here for the emission of the  $\text{Ph}^-$  ions via large cluster bombardment [14–16]. It may be recalled that keV sputtering produces secondary ions with different kinetic energies. The same must hold for single projectile impact. Given the kinetic energy spread, we assume that species with larger energies are more effectively ionized. It follows that the fraction of ejecta that are more energetic, i.e., that are more effectively ionized, contains the co-emitted ions. A more in-depth explanation would require knowledge of the kinetic energy distributions for the emitted neutral molecules. No such information is available to date.

A further question regarding multiple ion emission events, is the probability of emitting specified ion(s) as a function of the type of event. Fig. 4a and b shows the measured distributions,  $P(k_{\text{exp}}^-)$ , the number of  $\text{Ph}^-$  molecular ions detected per bombardment event. The observed distributions  $P(k_{\text{exp}}^-)$  for  $\text{Ph}^-$  molecular ions are different from the initial distribu-

tions  $P(k^-)$ , where  $k^-$  is the number of  $\text{Ph}^-$  ions emitted per event. From the measured distribution  $P(k_{\text{exp}}^-)$  obtained with the 8-anode detector we can calculate the initial distribution of the number of  $\text{Ph}^-$  ions:

$$P(k_{\text{exp}}^-) = \sum_{p=0}^{k_{\text{exp}}^-} \left[ \Psi(p|k_{\text{exp}}^-) \sum_{k^- = 0}^p \Phi(k^-|p) P(k^-) \right] \quad (1)$$

The conditional probabilities  $\Psi(p|k_{\text{exp}}^-)$  and  $\Phi(k^-|p)$  are defined as:

$$\Psi(p|k_{\text{exp}}^-) = \frac{m!}{(m - k_{\text{exp}}^-)! (k_{\text{exp}}^-)!} \sum_{i=0}^{k_{\text{exp}}^-} (-1)^i \frac{(k_{\text{exp}}^-)!}{i! (k_{\text{exp}}^- - i)!} \times \left( 1 - \frac{m - k_{\text{exp}}^- + i}{m} \right)^p \quad (2)$$

$$\Phi(k^-|p) = \tau^p (1 - \tau)^{k^- - p} \frac{k^-!}{(k^- - p)! p!} \quad (3)$$

where  $m$  is the number of anodes (in our case  $m = 8$ ),  $\tau$  is a detection and transmission efficiency for  $\text{Ph}^-$  molecules. In our case the value of  $\tau$  is a constant for a given mass ( $\tau \sim 0.4$  for  $\text{Ph}^-$  molecules) regardless of the projectile used,  $\text{Au}_9^+$  or  $\text{Au}_{400}^{4+}$ . The methodology used is that of the occupancy theory [17]. In this approach secondary ions emitted from a single impact event, strike the MCP in a random and independent fashion. The electron pulses generated by the MCP are detected by an anode(s), again, randomly and independently. There is no restriction on pulses or anodes, i.e., it is possible for all pulses to strike a single anode or any combination of the eight. We assume random and independent detection since the experiments are ran in the event by event bombardment/detection mode. The frequency of bombardment is low ( $\sim 1000$  event/s), therefore the interference of ions detected from different events is negligible. All eight anodes are equivalent (central symmetry [7]). The relative difference in efficiency of detection for the different anodes was found to be  $< 10\%$ .

It may be noted that the experimental condition for the simultaneous detection of multiple  $\text{Ph}^-$  ions is that they have relative radial velocities corresponding to energies  $> 0.1$  eV. The distribution per projectile for the emitted  $\text{Ph}^-$  secondary ions  $P(k^-)$  is related to the total distribution per projectile of the emitted  $\text{Ph}$  molecules  $P(k)$  by:

$$P(k^-) = \sum_k \Omega(k|k^-) P(k) \quad (4)$$

The conditional probability  $\Omega(k|k^-)$  is defined as:

$$\Omega(k|k^-) = [\alpha(E, k^-)]^{k^-} [1 - \alpha(E, k^-)]^{k - k^-} \frac{k!}{(k - k^-)! k^-!} \quad (5)$$

where  $k$  is a number of the molecules emitted per event. The effective ionization probability for multi-ion emission event



is given by  $\alpha(E, k^-) = \alpha_1 (1 + (\Delta E/E)k^-)^z$  where  $\alpha_1$  is an effective ionization probability for the single ion emitted per event. The parameter  $z$  describes the dependence of the ionization probability  $\alpha(E)$  on the kinetic energy of the emitted particles  $\alpha \propto E^z$  [13–15].

From the experimental distribution for molecular ions we can infer the initial distribution of emitted molecules (neutral and ionized) and thus gain insight into the “reproducibility” of individual emission events. It has been shown by simulation in the case of atomic projectiles that a two-parametric negative binomial distribution approximates best the distribution of sputtered atoms [18]. For low energy projectiles (100 eV) the distribution actually evolves from a broad, asymmetric to a symmetric Poisson-like distribution. For large cluster bombardment (15 keV  $C_{60}^+$  on Ag), the distribution of all sputtered particles calculated by the molecular dynamic simulation can be approximated by a narrow and symmetric distribution [19]. As an appropriate approximation, we use the Poisson distribution for  $P(k)$ , which is given by  $P(k) = (Y^k/k!) \exp(-Y)$  where  $Y = \sum_k k P(k)$  is the yield of the Ph molecules. As mentioned above, the experimental distributions,  $P(k_{\text{exp}}^-)$ , are shown in Fig. 4a for the case of 28.6 keV  $Au_9^+$  and Fig. 4b for the case of 134.6 keV  $Au_{400}^{4+}$  bombardment. We present here also the calculated distributions,  $P(k^-)$ , and  $P(k)$  using the following values:  $Y\alpha_1 = 0.16$  (28.6 keV  $Au_9^+$ ),  $Y\alpha_1 = 1.24$  (134.6 keV  $Au_{400}^{4+}$ ) and  $z = 1$ . It should be noted that the ionization probability and yield are unknown parameters but the trend of the distribution  $P(k_{\text{exp}}^-)$  depends on the product  $Y\alpha_1$  regardless the absolute values of  $\alpha_1$  and  $Y$ . The parameters  $Y\alpha_1$  and  $z$  were determined by means of least-squares fit of the distribution  $P(k_{\text{exp}}^-)$ . We tested the latter by varying  $z$  from 0.5 to 2. Surprisingly, the most appropriate value for  $z$  is unity for both projectiles,  $Au_9^+$  and  $Au_{400}^{4+}$  within the framework of our approach (Eqs. (1)–(5) and Poisson distribution for  $P(k)$ ). Thus the ionization probability is a linear function ( $\alpha \propto E$ ) of the kinetic energy of the emitted molecules. This relationship holds within the experimental conditions studied which cover quite different projectile characteristics. The mechanism of the ionization of the emitted intact molecules remains to be further explored.

#### 4. Conclusions

The ejecta from the bombardment regimes considered here have several fundamental characteristics.  $Au_{400}^{4+}$  generates abundant multi-ion emission. The absence of Coulomb interactions among co-emitted ions shows that each evolves in a distinct space, or possibly time, domain. While there are no

“exit” conditions for the ensemble of ionized ejecta, there are for coincidentally emitted isobars, which are more energetic than when the same mass ion is detected alone. We infer from the distributions of the number of molecular ions emitted per event a Poisson distribution for the neutral molecules as predicted by MD simulations. Finally, the experimental confirmation of the Poisson-like distribution signifies that the impacts of a given large or massive projectile always result in equivalent emission events.

#### Acknowledgements

This work was funded by the NSF (CHE-0449312) and the R. A. Welch Foundation (A-1482).

#### References

- [1] S. Della-Negra, D. Jacquet, I. Lorthiois, Y. Le Beyec, O. Becker, K. Wien, *Int. J. Mass Spectrom.* 53 (1983) 215.
- [2] K.B. Ray, M.A. Park, E.A. Schweikert, *Nucl. Instrum. Methods Phys. Res. B* 82 (1993) 317.
- [3] R.A. Zubarev, I.S. Bitensky, P.A. Demirev, B.U.R. Sundqvist, *Nucl. Instrum. Methods Phys. Res. B* 88 (1994) 143.
- [4] R.D. Rickman, S.V. Verkhoturov, E.S. Parilis, E.A. Schweikert, *Phys. Rev. Lett.* 92 (2004), 047601/1.
- [5] R.D. Rickman, S.V. Verkhoturov, S. Balderas, N. Bestaoui, A. Clearfield, E.A. Schweikert, *Appl. Surf. Sci.* 231–232 (2004) 106.
- [6] S. Bouneau, S. Della-Negra, J. Depauw, D. Jacquet, Y. Le Beyec, J.P. Mouffron, A. Novikov, M. Pautrat, *Nucl. Instrum. Methods Phys. Res. B* 225 (2004) 579.
- [7] R.D. Rickman, S.V. Verkhoturov, G.J. Hager, E.A. Schweikert, J.A. Bennet, *Int. J. Mass Spectrom.* 241 (2005) 57.
- [8] S.V. Verkhoturov, E.A. Schweikert, *Anal. Bioanal. Chem.* 373 (7) (2002) 609.
- [9] T.A. Carlson, in: N.H. Tolk, M.M. Traum, J.C. Tully, T.E. Madey (Eds.), *Desorption Induced by Electronic Transitions: DIET I*, Springer-Verlag, Berlin, 1983, p. 169.
- [10] A.N. Markevitch, D.A. Romanov, S.M. Smith, R.J. Levis, *Phys. Rev. Lett.* (2004), 92 063001/1.
- [11] S.V. Verkhoturov, E.A. Schweikert, V. Chechik, R.C. Sabapathy, R.M. Crooks, E.S. Parilis, *Phys. Rev. Lett.* 87 (2001), 037601/1.
- [12] Z. Postawa, B. Czerwinski, M. Szewczyk, E.D. Smiley, N. Winograd, B.J. Garrison, *J. Phys. Chem. B* 108 (2004) 7831.
- [13] M.L. Yu, in: R. Behrisch, K. Wittmaack (Eds.), *Sputtering by Particle Bombardment III*, Springer-Verlag, Berlin, 1991, p. 91.
- [14] P. Williams, *Appl. Surf. Sci.* 13 (241) (1982).
- [15] A.R. Krauss, D.M. Gruen, *Surf. Sci.* 92 (14) (1980).
- [16] M.L. Yu, K. Mann, *Phys. Rev. Lett.* 57 (1476) (1986).
- [17] J. Riordan, *An Introduction to Combinatorial Analysis*, John Wiley & Sons Inc., New York, London, 1958, p. 90.
- [18] W. Eckstein, *Computer Simulation of Ion-Solid Interactions*, Springer-Verlag, Berlin, 1991, p.211.
- [19] Z. Postawa, B. Czerwinski, M. Szewczyk, E.D. Smiley, N. Winograd, B.J. Garrison, *Anal. Chem.* 75 (2003) 4402.